10.1098/rspa.2002.1013

THE ROYAL SOCIETY

Waveguide modes in elastic rods

BY ATUL BHASKAR

School of Engineering Sciences, Aeronautics and Astronautics, University of Southampton, Highfield, Southampton SO17 1BJ, UK

Received 9 October 2001; revised 16 April 2002; accepted 29 April 2002; published online 14 November 2002

This paper is concerned with wave propagation in elastic rods of cross-sectional shapes that admit coupling between bending and torsional motions. Dispersion relations for progressive and evanescent waves are presented in closed form. The general case of triple coupling and the special case of double coupling are considered. The propagation characteristics are analytically presented in the limits of the long and the short waves. Waveguide modes in these limits are presented as asymptotic expansions. The polarization behaviour in various regimes of propagation is studied. Eigenvalue veering is observed for coupled modes. For the complete spectrum involving complex wavenumber, the problem of obtaining the dispersion relation and the propagation modes is cast as a standard eigenproblem. Illustrative examples are given.

Keywords: elastic waves; dispersion; bending–torsion coupling; asymptotic analysis; eigenvalue veering

1. Introduction

Thin elastic rods are frequently used in engineering constructions. The dynamic behaviour of these structural elements can be studied by the method of normal modes or by wave-propagation techniques. This paper is concerned with the latter. When the wavelengths of interest are considerably longer than the typical cross-sectional dimensions, and when the bending deformations are decoupled from the twisting deformation of the cross-section, there are three well-known wave types that an elastic waveguide can support: axial waves, torsional waves and bending waves. Bending deformations are decoupled from the torsional deformations when the kinetic and potential energy expressions do not contain terms that are bilinear in the relevant coordinates (i.e. transverse displacements and cross-sectional rotation about the longitudinal axis) or their time derivatives. This happens when the cross-section possesses two axes of symmetry (these two axes coincide with the principal axes of the cross-section and the second moment of area tensor is diagonal). Of the three waves that can propagate in such a medium, the axial waves and torsional waves are non-dispersive, whereas the bending waves are dispersive. For non-dispersive propagation, the frequency ω is proportional to the wavenumber k, so that the group velocity $\partial\omega/\partial k$ is independent of k. These classical cases are well-documented in the standard texts (see, for example, Graff 1975).

In this paper, we are concerned with the torsional and the bending propagation modes only; the axial deformations decouple from the cross-sectional displacement field under the assumptions of linear elasticity. In particular, wave motion will be studied when the symmetry of the cross-sectional shape does not decouple bending deformations from the torsional ones. When this happens, the centroid and the shear centre of the cross-section do not coincide. The field equations for a general coupling of the bending and the torsional motions were presented by Timoshenko (1955). Later, Gere & Lin (1958) and Lin (1960) studied the vibration characteristics of open-section channels having coupled torsion and bending using Rayleigh–Ritz method. Bishop & Price (1977) included the effect of shear deformation and rotary inertia for the coupled bending–torsion problem. Dokumaci (1987) presented exact natural frequencies for beams with single cross-sectional symmetry. This was further generalized by Bishop *et al.* (1989), who included the effect of warping. Bishop *et al.* (1985) presented a comparison of various beam theories.

All the studies cited above are limited to the normal-mode vibration of beams of finite extent. The wave-propagation problem in an infinitely long medium is fundamental to the study of dynamics and is algebraically simpler to handle (as compared with free vibration problem for beams of finite length). In view of these, it is surprising that an analytical study that brings out the qualitative behaviour of the dispersion characteristics in various regimes of propagation is not yet available in the literature. The purpose of this paper is to provide this fundamental understanding.

It is only recently that, in an interesting study, Yaman (1997) used wave propagation techniques to study the forced vibration of rods of finite length as well as that of rods of semi-infinite extent (rods that extend in one direction). He obtained an eighth-order algebraic equation with wavenumber as the unknown when bending and torsion are doubly coupled. When triple coupling exists, the corresponding equation is 12th order. He identified two branches of the dispersion curve (for propagating waves): one that is 'predominantly flexural but with some torsion' and one that is 'predominantly torsional with some bending' for doubly coupled rods. For triple coupling, he inferred the existence of a 'torsional wave with bi-directional flexural properties' and two branches that are 'predominantly flexural but with some torsion'. Although this classification of the dispersion curves is intuitively appealing, a careful analysis presented in this paper will reveal a different story.

If we seek admissible wavenumber values for a prescribed frequency value (as in Yaman 1997), the formulation does not admit an easy analysis for studying propagation behaviour. Of course, if the objectives are primarily to *compute* the dispersion relation, the approach is perfectly satisfactory. On the other hand, if we posed the problem as one of determining the admissible *frequency for a prescribed wavenumber*, the dispersion relation $\omega(k)$ can be obtained in closed form and simple analyses could be performed for different limiting values of (real or imaginary) wavenumber (i.e. for purely propagating and evanescent waves).

This paper is organized as follows. Solutions for the propagating waves and for the evanescent waves are presented in closed form for double coupling and for triple coupling in § 2. Asymptotic analyses for dispersion behaviour and waveguide modes in the limits of long waves and short waves are presented in § 3. Polarization behaviour is also studied in this section. The cases of complex wavenumber with and without damping are presented in terms of appropriate eigenvalue problems in § 4. Illustrative examples are given in § 5.

2. Field equations and dispersion relations

We use the notations of Gere & Lin (1958). For a beam of length l extending in the x-direction, the potential energy functional is given by

$$U = \frac{EI_\zeta}{2}\int_0^l (v'')^2\,\mathrm{d}x + \frac{EI_\eta}{2}\int_0^l (w'')^2\,\mathrm{d}x + \frac{EC_w}{2}\int_0^l (\phi'')^2\,\mathrm{d}x + \frac{GC}{2}\int_0^l (\phi')^2\,\mathrm{d}x. \quad (2.1)$$

Here E is the modulus of elasticity; I_ζ and I_η are the second moments of area about ζ- and η-axes (the principal directions of the cross-section); $v(x,t)$ and $w(x,t)$ are the bending displacements of the shear centre in the principal directions of the cross-section η and ζ, respectively, whereas $\phi(x,t)$ is the torsional rotation about the x-axis; G is the shear modulus; C_w is the warping constant; and C is the torsional stiffness of the cross-section. A prime denotes differentiation with respect to the spatial variable x. The potential-energy terms appear as sums of squares in variables v, w and ϕ, since ζ and η define the principal directions. If we chose any other coordinates, we would, in general, have potential energy terms that contain products of the field variables.

The kinetic energy functional is given by

$$T = \frac{\rho A}{2}\int_0^l (\dot v - \dot\phi c_z)^2\,\mathrm{d}x + \frac{\rho A}{2}\int_0^l (\dot w + \dot\phi c_y)^2\,\mathrm{d}x + \frac{\rho I_\mathrm{p}}{2}\int_0^l \dot\phi^2\,\mathrm{d}x, \quad (2.2)$$

where I_p is the polar moment of inertia of the cross-section about the centroid and (c_z, c_y) are the coordinates of the centroid in the principal cross-sectional directions (ζ,η) that pass through the shear centre of the cross-section. A dot represents differentiation with respect to time t. The terms $\dot v\dot\phi$ and $\dot w\dot\phi$ in the kinetic energy expression introduce coupling in the inertia terms. Using Hamilton's principle, the first variation of the time integral of the Lagrangian $L = T - U$ is set to zero, i.e. $\delta\int_{t_1}^{t_2} L\,\mathrm{d}t = 0$. Admissible variations must be co-terminus in space and time. After carrying out appropriate variations, the set of coupled partial differential equations

$$\left.\begin{aligned} \lambda_\zeta v'''' + \ddot v - c_z\ddot\phi &= 0,\\ \lambda_\eta w'''' + \ddot w + c_y\ddot\phi &= 0,\\ \lambda_w\phi'''' - \lambda_\mathrm{p}\phi'' - c_z\ddot v + c_y\ddot w + c_x\ddot\phi &= 0, \end{aligned}\right\} \quad (2.3)$$

is obtained, where

$$\lambda_\zeta = \frac{EI_\zeta}{\rho A}, \qquad \lambda_\eta = \frac{EI_\eta}{\rho A}, \qquad \lambda_\mathrm{p} = \frac{GC}{\rho A}, \qquad \lambda_w = \frac{EC_\mathrm{w}}{\rho A} \quad \text{and} \quad c_x = \frac{I_0}{\rho A}$$

and I_0 is the polar moment of area about the shear centre. Gere & Lin called these equations 'triply coupled', since they are a set of three partial differential equations that cannot be solved independently of each other. When either $c_y = 0$ or $c_z = 0$, one of the first two equations of the three equations in (2.3) decouples from the remaining two. This situation was described by Gere *et al.* as the case of double coupling. When $c_y = c_z = 0$, the three equations decouple from each other and can be solved independently. The resulting propagation behaviour is classical: one torsional wave and two bending waves are observed. The non-dispersive torsional wave has the frequency–wavenumber relationship given by $\omega^2 c_x = \lambda_\mathrm{p}k^2$ (when warping is ignored) and for the two dispersive bending waves it is given by $\omega^2 = \lambda_\zeta k^4$ and $\omega^2 = \lambda_\eta k^4$.

When a general state of coupling exists and when warping is included in the model, travelling-wave solutions for the three field variables (two transverse displacements and one torsion) must have the following spatio-temporal variation

$$\{v, w, \phi\}(x,t) = \{V, W, \Phi\} \exp\{\mathrm{i}(kx - \omega t)\}. \tag{2.4}$$

Substituting these into equations (2.3) and organizing the terms in a matrix form we have

$$\begin{bmatrix} (k^4\lambda_\zeta) & 0 & 0 \\ 0 & (k^4\lambda_\eta) & 0 \\ 0 & 0 & (k^4\lambda_w + k^2\lambda_\mathrm{p}) \end{bmatrix} \begin{Bmatrix} V \\ W \\ \Phi \end{Bmatrix} = \omega^2 \begin{bmatrix} 1 & 0 & -c_z \\ 0 & 1 & c_y \\ -c_z & c_y & c_x \end{bmatrix} \begin{Bmatrix} V \\ W \\ \Phi \end{Bmatrix}. \tag{2.5}$$

For a given real value of k, equation (2.5) is a generalized *symmetric* eigenproblem of the form $\boldsymbol{A}\boldsymbol{u} = \mu\boldsymbol{B}\boldsymbol{u}$ where $\mu = \omega^2$, $\boldsymbol{B}$ is the coefficient matrix on the right-hand side, and $\boldsymbol{A}(k)$ is a 3×3 diagonal matrix that depends on the wavenumber k. Equation (2.5) can be seen as the double Fourier transform of equations (2.3) in the frequency and wavenumber domains.

It can be verified that $\boldsymbol{B}$, the coefficient matrix on the right-hand side of (2.5), is positive definite since $(c_x - c_y^2 - c_z^2) = \rho^2$, where ρ is the radius of gyration of the cross-section and therefore, is always positive. The coefficient matrix $\boldsymbol{A}(k)$ is symmetric. Therefore, the generalized eigenproblem $\boldsymbol{A}\boldsymbol{u} = \mu\boldsymbol{B}\boldsymbol{u}$ yields real eigensolutions. For positive wavenumber k, $\boldsymbol{A}(k)$ is positive definite. In this case, the eigenvalues are positive, i.e. $\omega = \pm\sqrt{\mu}$ are real. Due to $\boldsymbol{A}(k)$ being an even function of k, changing k to $-k$ does not result in any change in $\boldsymbol{A}$. Therefore, for real wavenumber $\pm k$, real frequencies $\pm\omega$ result. These four solutions together constitute the complete set of propagating waves (there are three such sets, one for each value of μ) in the positive as well as the negative x-directions.

When k is imaginary, say $k = \pm\mathrm{i}\kappa$, $\boldsymbol{A}(\kappa)$ and $\boldsymbol{B}$ still remain symmetric, with $\boldsymbol{B}$ positive definite. The definiteness of $\boldsymbol{A}(\kappa)$, however, is not now guaranteed. This is due to the term $(\kappa^4\lambda_w - \kappa^2\lambda_\mathrm{p})$ on the third diagonal of $\boldsymbol{A}$. Negative values of μ, if any, need to be kept out of consideration, since they correspond to imaginary frequencies. Indeed, one is free to choose which, if any, of ω and k shall be real. Here we have chosen ω to be real so that the time variation in $\exp\mathrm{i}(kx - \omega t)$ is constant in amplitude. Positive values of μ correspond to $\omega = \pm\sqrt{\mu}$ as before and the solution $\exp(\pm kx \pm \mathrm{i}\omega t)$ represents evanescent waves for negative and positive x.

The eigenproblem (2.5) can be expressed as

$$\boldsymbol{D}(k,\omega)\boldsymbol{u} = \boldsymbol{0}. \tag{2.6}$$

The existence of non-trivial solutions requires $\det[\boldsymbol{D}(k,\omega)] = D(k,\omega) = 0$. The determinant $D(k,\omega)$ can be identified as the dispersion function, which is well-known in the wave propagation literature. It describes the relationship between the wavenumber and the frequency, such that a spatially and temporally harmonic solution is feasible. For purely propagating waves, ω and k are both real. For evanescent waves, ω is real and k is purely imaginary. For the ith non-trivial value ω_i, the corresponding $\boldsymbol{u}_i$ describes a waveguide mode.

The dispersion relation is a cubic algebraic equation in terms of the square of the frequency, ω^2 (as opposed to 12th order in terms of the wavenumber k as in Yaman

(1997)) and therefore admits closed-form solutions. Expanding the determinant, we have

$$a\mu^3 + b\mu^2 + c\mu + d = 0, \tag{2.7}$$

where $a = (c_x - c_y^2 - c_z^2)$, $b = (c_y^2 k_v + c_z^2 k_w - k_\phi - k_v c_x - k_w c_x)$, $c = (k_v k_\phi + k_w k_\phi + k_v k_w c_x)$ and $d = -k_v k_w k_\phi$ and where $\mu = \omega^2$. The parameters k_v, k_w and k_ϕ are constants in the above cubic for specified values of the wavenumber k and are given by $k_v = k^4\lambda_\zeta$, $k_w = k^4\lambda_\eta$ and $k_\phi = k^4\lambda_w + k^2\lambda_\mathrm{p}$. The solution of equation (2.7) gives the relationship between ω and k for all propagating waves.

The cubic equation (2.7) can be solved in many ways, the method of Cardano being perhaps the best known. Following a more recent approach (Nickalls 1993), the three roots are given by

$$[\alpha, \beta, \gamma] = x_N + 2\delta\cos[\theta, (2\pi/3 + \theta), (4\pi/3 + \theta)], \tag{2.8}$$

where $x_N = -b/(3a)$, $\delta^2 = (b^2 - 3ac)/9a^2$, $\cos 3\theta = -y_N/h$, $y_N = ax_N^3 + bx_N^2 + cx_N + d$, and $h = 2a\delta^2$. It can be shown that a cubic that requires four parameters for its description has x_N, y_N, δ, and h as these parameters in lieu of a, b, c, and d as in (2.7).

All the evanescent waveguide modes can be computed in a manner similar to the propagating waves by substituting $k = \mathrm{i}\kappa$ into equation (2.5). This substitution leads to the dispersion relations for evanescent waves which reads as $D(\kappa, \omega) = 0$, resulting in the cubic equation

$$a'\mu^3 + b'\mu^2 + c'\mu + d' = 0. \tag{2.9}$$

The coefficients a', $b'(\kappa)$, $c'(\kappa)$ and $d'(\kappa)$ are given by $a' = a$, $b' = (c_y^2\kappa_v + c_z^2\kappa_w - \kappa_\phi - \kappa_v c_x - \kappa_w c_x)$, $c' = (\kappa_v\kappa_\phi + \kappa_w\kappa_\phi + \kappa_v\kappa_w c_x)$ and $d' = -\kappa_v\kappa_w\kappa_\phi$. Here $\kappa_v = \kappa^4\lambda_\zeta$, $\kappa_w = \kappa^4\lambda_\eta$, and $\kappa_\phi = \kappa^4\lambda_w - \kappa^2\lambda_\mathrm{p}$. Each positive value of k corresponds to three positive values of ω, leading to three branches of the dispersion relation on the ω–k plane. This cubic equation is also solved in closed form by using the approach of equation (2.8).

When the cross-sectional plane has one axis of symmetry (say the y-axis), then $c_z = 0$ and the 'v equation' (the first of the three in equation (2.3)) decouples from the remaining two. In this case the dispersion relation is given by a quadratic in ω^2,

$$(c_x - c_y^2)\omega^4 - (k_w c_x + k_\phi)\omega^2 + k_w k_\phi = 0, \tag{2.10}$$

whose two roots

$$\omega_{(1,2)}^2 = \frac{(k_w + k_\phi) \pm \sqrt{(k_w - k_\phi)^2 + 4k_w k_\phi c_y^2}}{2(c_x - c_y^2)} \tag{2.11}$$

correspond to the two branches of the dispersion curve. The third branch is a decoupled classical bending wave. For evanescent waves, closed-form solutions are obtained by substituting k_v, k_w, k_ϕ by κ_v, κ_w, and κ_ϕ, respectively.

3. Asymptotic dispersion behaviour and polarization of waves

While the cubic equation (2.7) and the quadratic (2.10) can be solved in the closed form as, in equations (2.8) and (2.11), respectively, the limiting behaviour of the dispersion relations for long waves and short waves can be better understood by

asymptotic analyses. The long-wavelength behaviour will be studied first. The two cases of double coupling and triple coupling will be taken-up in turn.

When there is one axis of symmetry in the cross-section (say the y-axis), one of the two offsets between the cross-sectional centroid and the shear centre is zero (i.e. $c_z = 0$). For long waves, $\epsilon = k^2$ is small and the eigenvalues μ are given by

$$\mu^2(c_x - c_y^2) - (c_x\lambda_\eta\epsilon^2 + \lambda_\mathrm{p}\epsilon)\mu + \lambda_\eta\lambda_\mathrm{p}\epsilon^3 = 0, \tag{3.1}$$

when warping is ignored. Instead of solving the quadratic for μ, we can develop an asymptotic expansion for small wavenumber (i.e. for small ϵ) as

$$\mu = \epsilon\mu_1 + \epsilon^2\mu_2 + \epsilon^3\mu_3 + \ldots. \tag{3.2}$$

The leading term does not contain ϵ^0 since $\mu(\epsilon)$ passes through the origin (this is confirmed by substituting $\epsilon = 0$ in equation (3.1)). This means that the two branches of the dispersion curve do not have any cut-on frequency. Collecting like powers of ϵ and setting the coefficient terms to zero (this is equivalent to dividing throughout by appropriate powers of ϵ and letting $\epsilon \to 0$ successively (see Nayfeh 1973)) results in the unknown coefficients μ_1, μ_2, μ_3, etc. The two branches of the dispersion curve are given by

$$\left.\begin{aligned} \omega_{(1)}^2 &= \lambda_\eta k^4 - \left(\frac{\lambda_\eta^2 c_y^2}{\lambda_\mathrm{p}}\right)k^6 + O(k^8), \\ \omega_{(2)}^2 &= \left(\frac{\lambda_\mathrm{p}}{c_x - c_y^2}\right)k^2 + \left(\frac{\lambda_\eta c_y^2}{c_x - c_y^2}\right)k^4 + \left(\frac{\lambda_\eta^2 c_y^2}{\lambda_\mathrm{p}}\right)k^6 + O(k^8). \end{aligned}\right\} \tag{3.3}$$

Note in the above asymptotic expansions that the leading term in the first expression is $\lambda_\eta k^4$ and that it is $\lambda_\mathrm{p}k^2/(c_x - c_y^2)$ in the second. Therefore, there is one dispersive propagation mode and one non-dispersive propagation mode in the limit of long waves. These two could be compared with the classical beam-bending and torsional dispersion relations that have the general functional forms $\omega \sim k^2$ and $\omega \sim k$ respectively. Despite a non-dispersive ('torsion-like') dependence of frequency on wavenumber, we shall see later that it is rash to conclude that the second branch is torsional in the limit of long waves.

The propagation behaviour in the limit of short waves can be studied by casting the dispersion function as

$$\mu^2(c_x - c_{y^2})\epsilon'^3 - (c_x\lambda_\eta\epsilon' + \lambda_\mathrm{p}\epsilon'^2)\mu + \lambda_\eta\lambda_\mathrm{p} = 0, \tag{3.4}$$

where $\epsilon' = (1/k^2) \to 0$ as $k \to \infty$. Since the leading term in the equation involves the small parameter ϵ', the case of short waves is a problem of *singular perturbation*, indicating that we need to include terms such as ϵ'^{-m}, with $m > 0$ in the expansion. With some trial it is found that an expansion of the form

$$\mu = \frac{\mu_{-2}}{\epsilon'^2} + \frac{\mu_{-1}}{\epsilon'} + \mu_0 + \ldots \tag{3.5}$$

is appropriate. Going through steps similar to those following equation (3.2), we obtain the following expansion for short waves

$$\left.\begin{aligned} \omega_{(1)}^2 &= \left(\frac{\lambda_\mathrm{p}}{c_x}\right)k^2 - \left(\frac{\lambda_\mathrm{p}^2 c_y^2}{c_x^3\lambda_\eta}\right) + O\left(\frac{1}{k^2}\right), \\ \omega_{(2)}^2 &= \left(\frac{c_x\lambda_\eta}{c_x - c_y^2}\right)k^4 + \left[\frac{\lambda_\mathrm{p}c_y^2}{c_x(c_x - c_y^2)}\right]k^2 + \left(\frac{\lambda_\mathrm{p}^2 c_y^2}{c_x^3\lambda_\eta}\right) + O\left(\frac{1}{k^2}\right). \end{aligned}\right\} \tag{3.6}$$

We then compare the leading-order terms of equations (3.3) and (3.6). Recall that $c_x = I_0/A$, where I_0 is the second moment of area about an axis passing through the shear centre; it follows that $(c_x - c_y^2) = \rho^2$, where ρ is the radius of gyration of the cross-section. Since the inertia forces effectively act through the centroid of the cross-section, pure bending and pure torsion modes would have dispersion relations as $\omega_{\mathrm{B}}^2 \sim \lambda_\eta^2 k^4$ and $\omega_{\mathrm{T}}^2 \sim (\lambda_{\mathrm{p}}/c_x)^2 k^2$. Therefore, from equations (3.3) and (3.6), it follows that, for long waves, bending waves have a higher-order effect due to coupling with torsional deformation, and the torsional mode for short waves has a higher-order effect due to coupling with bending deformation. On the other hand, the 'torsional mode' for long waves has a leading-order effect due to coupling with bending deformations and 'bending mode' for short waves has a leading-order effect due to coupling with torsional deformation. An explanation of this requires the knowledge of waveguide mode shape; discussion on this is postponed for the moment (note the quotes on the two occasions in the previous statement, we will come back to this shortly).

When cross-sectional warping is admitted in the model the first equation in (3.3) remains unchanged, whereas the second equation gets modified such that its second term becomes $(\lambda_\eta c_y^2 + \lambda_w)/(c_x - c_y^2)$. This means that, for long waves, warping does not couple0 with the bending branch of the dispersion equation, whereas the predominantly non-dispersive branch has a second-order effect, as expected. For short waves, the torsional branch is dominated by warping. Therefore, we do not expect minor changes due to the introduction of warping at large wavenumber. The singular perturbation problem (3.4) is now modified to

$$\mu^2(c_x - c_{y^2})\epsilon'^4 - (c_x\lambda_\eta\epsilon'^2 + \lambda_{\mathrm{p}}\epsilon'^3)\mu + \lambda_\eta\lambda_{\mathrm{p}}\epsilon' + \lambda_\eta\lambda_w. \tag{3.7}$$

Note that the leading singular term in the equation is affected when the warping mechanism of deformation is incorporated into the model. The dominant behaviour in the limit of short waves is then given by

$$\omega_{(1,2)}^2 = \left[\frac{(c_x\lambda_\eta + \lambda_w) \pm \sqrt{(c_x\lambda_\eta - \lambda_w)^2 + 4\lambda_\eta\lambda_w c_y^2}}{2(c_x - c_y^2)}\right] k^4 + O(k^2). \tag{3.8}$$

This indicates that, for short waves, *both* the branches of the dispersion curve have the functional form $\omega^2 \sim k^4$, because warping dominates for the torsional wave rendering it dispersive for large wavenumber. When λ_w approaches zero in the above equation, $O(k^4)$ term vanishes for one branch and we are left with only the $O(k^2)$ term, which is consistent with equation (3.6). If we use $c_y = 0$ instead of $c_z = 0$, the analysis of equations (3.1)–(3.8) is analogous. A new set of equations is obtained by replacing c_y by c_z and λ_η by λ_ζ throughout.

Having examined the limiting cases, we can rule out certain regions in the ω–k plane for the admissible values that allow wave propagation. To do this, the dispersion function can be reorganized as

$$f(\tilde{\mu}) = (B - \tilde{\mu})(C - \tilde{\mu}) - EG = 0, \tag{3.9}$$

where

$$\tilde{\mu} = \frac{1}{\omega^2}, \qquad B(k) = \frac{1}{k^4\lambda_\eta}, \qquad C(k) = \frac{c_x}{k^2\lambda_{\mathrm{p}}}, \qquad E(k) = \frac{c_y}{k^4\lambda_\eta}, \qquad G(k) = \frac{c_y}{k^2\lambda_{\mathrm{p}}}.$$

Noting the following properties of the expression on the left-hand side,

(i) as $\tilde{\mu} \to \infty$, $f(\tilde{\mu}) \to +\infty$,

(ii) $f(0) = BC - EG > 0$,

(iii) $f(B) < 0$,

(iv) $f(C) < 0$, and

(v) as $\tilde{\mu} \to -\infty$, $f(\tilde{\mu}) \to +\infty$,

we conclude that there is one root of $f(\tilde{\mu})$ in the range $0 \leqslant \tilde{\mu} \leqslant B$ and one root in the range $B \leqslant \tilde{\mu} \leqslant \infty$, whereas there is no root in the range (B, C). Examining the expressions for B and C, it follows that no portion of the curves $\omega_{(1,2)}(k)$ must fall in the regions enclosed by

$$\hat{\omega}_{(1)}(k) = \sqrt{\lambda_\eta} k^2 \quad \text{and} \quad \hat{\omega}_{(2)}(k) = \left(\sqrt{\lambda_\mathrm{p}/c_x}\right) k :$$

the two classical dispersion curves had there been no bending–torsion coupling. Similarly, it can be shown that

(vi) $f(B') < 0$ and

(vii) $f(C') < 0$,

where $B' = (c_x - c_y^2)/(c_x \lambda_\eta k^4)$ and $C' = (c_x - c_y^2)/(\lambda_\mathrm{p} k^2)$. Since $\tilde{\mu} > 0$ does not fall in the range $(\min[B, B', C, C'], \max[B, B', C, C'])$, it follows that $\mu = 1/\tilde{\mu}$ does not fall in the range $(\min[1/B, 1/B', 1/C, 1/C'], \max[1/B, 1/B', 1/C, 1/C'])$. Therefore, noting (ii) and (v), it follows that one branch of the dispersion curve is always *above* all the four curves

$$C_1 : \omega = \sqrt{\lambda_\eta} k^2, \qquad C_2 : \omega = \sqrt{\frac{\lambda_\mathrm{p}}{c_x}} k,$$

$$C_3 : \omega = \sqrt{\frac{\lambda_\eta c_x}{(c_x - c_y^2)}} k^2, \qquad C_4 : \omega = \sqrt{\frac{\lambda_\mathrm{p}}{(c_x - c_y^2)}} k,$$

and one branch is always *below* all these four curves. It also means that the two branches of the dispersion relation are non-intersecting. Since C_3 is always above C_1, C_2 is always above C_4 and the straight lines are above the parabolas for small k, whereas the parabolas are above the straight lines for large k (at intermediate values of k, the ordering is complicated), it further follows that *the branch that is non-dispersive for small k passes through a transition and becomes dispersive for large k*. On the other hand, *the branch that starts as being dispersive for long waves becomes non-dispersive for short waves*. The understanding of the propagation modes requires knowledge of the eigenvectors and will be discussed later.

The case of triple coupling is taken up now. For small wavenumber (long waves), the 3×3 eigenproblem (2.5) becomes

$$\tilde{a}\mu^3 + (\tilde{b}\epsilon^2 + \tilde{c}\epsilon)\mu^2 + (\tilde{d}\epsilon^3 + \tilde{e}\epsilon^4) + \tilde{f}\epsilon^5 = 0, \tag{3.10}$$

where $\tilde{a} = (c_x - c_y^2 - c_z^2)$, $\tilde{b} = \lambda_\eta c_z^2 + \lambda_\zeta c_y^2 - c_x(\lambda_\zeta + \lambda_\eta)$, $\tilde{c} = -\lambda_\mathrm{p}$, $\tilde{d} = \lambda_\mathrm{p}(\lambda_\zeta + \lambda_\eta)$, $\tilde{e} = \lambda_\zeta \lambda_\eta c_x$ and $\tilde{f} = \lambda_\zeta \lambda_\eta \lambda_\mathrm{p}$. The small parameter ϵ is defined as $\epsilon = k^2$, as before.

To work out a particle trajectory during wave propagation, consider two mutually orthogonal planes that intersect in the longitudinal direction such that the longitudinal axis is formed by joining the shear centres of each cross-section. The orientation of these planes about the longitudinal axis is such that they contain the principal directions of the cross-section. Looking into the longitudinal axis along the propagation direction, the longitudinal axis will have deflections $v(x,t)$ and $w(x,t)$. The trajectory of a particle on the longitudinal axis in a plane perpendicular to the longitudinal axis, as can be seen from equation (3.15), will be a straight line with a fixed orientation with respect to the principal directions of the cross-section (for a given k). Therefore, the propagation is *plane polarized*. The tangent of the angle between the plane of polarization and the planes that contain a principal axis is given by the expression $V_{\mathrm{i}}/W_{\mathrm{i}}$.

If the bending modes about the two principal directions of the cross-section are degenerate, a linear combination of the degenerate modes is also a valid mode. In that situation, apart from plane-polarized propagation, *circularly polarized* propagation (or more generally, elliptically polarized since we are superposing two orthogonal sinusoidal motions) is also possible. Examples of cross-sectional shapes that support such waves include squares, equilateral triangles or any regular polygon. Indeed, the circular cross-section has an infinite-fold degeneracy. Such propagation behaviour is well known in other branches of physics (e.g. electromagnetism/optics).

To examine if pure bending or torsional motions are at all possible, we can substitute $v = 0$ and $\phi = 0$ or $w = 0$, in turn, in the kinetic and potential energy expressions. In the first instance, they are given by

$$T = \tfrac{1}{2}\rho A \int \dot{w}^2 \,\mathrm{d}x \quad \text{and} \quad V = \tfrac{1}{2} E I_\eta \int (w'')^2 \,\mathrm{d}x,$$

respectively, leading to the dispersion relation $\omega^2 = \lambda_\eta k^4$. Similarly, it can be checked from the energy expressions that it is a requirement for propagating pure torsional motion (for particular wavenumber–frequency combinations, even when coupling may generally exist between bending and torsion motions) that the dispersion relation must be of the form $\omega^2 = (\lambda_{\mathrm{p}}/c_x)k^2$ in the absence of warping. This indicates that the second dispersion relation in (3.3) does not correspond to a torsional mode (despite an asymptotically non-dispersive behaviour for long waves) and the second dispersion relation in (3.6) does not mean a bending behaviour despite an asymptotically parabolic $\omega(k)$ relationship. More detailed statements regarding cross-sectional motion require further analysis, which follows.

It is possible to obtain asymptotic expansions for the mode shapes to determine the dominant features of the cross-sectional displacement in a waveguide mode. Using equation (3.14) and the expansions of equation (3.3) for long waves, we obtain the two mode shapes as

$$\frac{\Phi_1}{W_1} = \left(\frac{\lambda_\eta c_y}{\lambda_{\mathrm{p}}}\right) k^2 + O(k^4), \qquad \frac{W_2}{\Phi_2} = -c_y + \frac{c_y(c_x - c_y^2)\lambda_\eta}{\lambda_{\mathrm{p}}} k^2 + O(k^4). \tag{3.16}$$

In the limit $k \to 0$ (long waves), noting that scaling for eigenvectors can be chosen arbitrarily,

$$\lim_{k\to 0} \begin{Bmatrix} W \\ \Phi \end{Bmatrix}_{(1,2)} = \begin{Bmatrix} 1 \\ 0 \end{Bmatrix}, \begin{Bmatrix} -c_y \\ 1 \end{Bmatrix}. \tag{3.17}$$

It is seen that μ has a triple root at the origin, indicating that the three branches of the dispersion curve do not have any cut-on frequency. Assuming an asymptotic expansion of the form (3.2), we have three branches of the dispersion relations for long waves. The first two branches, described by

$$\omega_{(1)}^2 = \lambda_\eta k^4 - \left(\frac{\lambda_\eta^2 c_y^2}{\lambda_\mathrm{p}}\right)k^6 + O(k^8), \qquad \omega_{(2)}^2 = \lambda_\varsigma k^4 - \left(\frac{\lambda_\varsigma^2 c_z^2}{\lambda_\mathrm{p}}\right)k^6 + O(k^8), \quad (3.11)$$

can be viewed as perturbations on the classical bending dispersion relations $\hat{\omega}_{(1)} \sim \sqrt{\lambda_\eta}k^2$ and $\hat{\omega}_{(2)} \sim \sqrt{\lambda_\varsigma}k^2$. The third branch,

$$\omega_{(3)}^2 = \left(\frac{\lambda_\mathrm{p}}{c_x - c_y^2 - c_z^2}\right)k^2 + \left(\frac{\lambda_\varsigma c_z^2 + \lambda_\eta c_y^2}{c_x - c_y^2 - c_z^2}\right)k^4 + \left(\frac{\lambda_\eta c_y^2 + \lambda_\varsigma c_z^2}{\lambda_\mathrm{p}}\right)k^6 + O(k^8), \quad (3.12)$$

is non-dispersive in the limit of long waves. However, we shall see later that it does not correspond to torsional motion. Compare (3.11) with the first equation in (3.3) and equation (3.12) with the second equation in (3.3); equation (3.3) can be recovered as a special case of (3.11) and (3.12).

For short waves, the regular perturbation problem (3.10) becomes singular in terms of the small parameter $\epsilon' = 1/\epsilon$, with the leading term multiplied by ϵ'^5. The algebra for determining the series of type (3.5) is complicated now, and the dominant terms of the expansion are given by

$$\left.\begin{aligned} \omega_{(1,2)}^2 &= \left[\frac{-\tilde{b} \pm \sqrt{\tilde{b}^2 - 4\tilde{a}\tilde{e}}}{2\tilde{a}}\right]k^4 + O(k^2), \\ \omega_{(3)}^2 &= \left(\frac{\lambda_\mathrm{p}}{c_x}\right)k^2 + O(k^0). \end{aligned}\right\} \quad (3.13)$$

So far we have been concerned with the propagation characteristics. The propagation modes can be interpreted from the relevant eigenvectors. The solution μ of the cubic equations (2.7) or (2.9) is real, and therefore the corresponding eigenvector $[V_\mathrm{i}, W_\mathrm{i}, \Phi_\mathrm{i}]^\mathrm{T}$ must be real. For each value of $\tilde{\mu} = \tilde{\mu}_\mathrm{i} = 1/\mu_\mathrm{i}$, equation (2.5) can be solved uniquely up to an arbitrary scaling of the eigenvector. The components of the ith eigenvector are given by

$$V_\mathrm{i} = \frac{c_z}{(1 - \tilde{\mu}_\mathrm{i}k_v)}, \qquad W_\mathrm{i} = \frac{-c_y}{(1 - \tilde{\mu}_\mathrm{i}k_w)}, \qquad \Phi_\mathrm{i} = 1. \quad (3.14)$$

The value of Φ_i has been arbitrarily set to unity for scaling of the eigenvector. These mode shapes depend on the value of the wavenumber through the dependence of k_v and k_w on k. The value of μ_i, of course, corresponds to this value of k through the dispersion relation $D(k, \omega) = 0$. For evanescent waves, the k are replaced by κ with the corresponding subscripts.

The relative magnitude of the transverse displacements depends linearly on the offsets c_z and c_y between the centroid and the shear centre. It is one of the benefits of the closed-form solution presented here that such parametric dependence can be known explicitly. The ratio of V_i to W_i is given by

$$\frac{V_\mathrm{i}}{W_\mathrm{i}} = -\frac{c_z(1 - \tilde{\mu}_\mathrm{i}k_w)}{c_y(1 - \tilde{\mu}_\mathrm{i}k_v)}. \quad (3.15)$$

Similarly, for short waves, after using the expansions (3.6) in (3.14), we obtain expressions for the eigenvectors as

$$\frac{W_1}{\Phi_1} = \left(\frac{\lambda_{\mathrm{p}} c_y}{\lambda_\eta c_x}\right)\frac{1}{k^2} + O\left(\frac{1}{k^4}\right), \qquad \frac{W_2}{\Phi_2} = -\left(\frac{c_x}{c_y}\right) + \frac{(c_x - c_y^2)\lambda_{\mathrm{p}}}{c_x c_y \lambda_\eta}\frac{1}{k^2} + O\left(\frac{1}{k^4}\right). \tag{3.18}$$

In the limit $k \to \infty$, we obtain the propagation modes

$$\lim_{k\to\infty} \begin{Bmatrix} W \\ \Phi \end{Bmatrix}_{(1,2)} = \begin{Bmatrix} 0 \\ 1 \end{Bmatrix}, \begin{Bmatrix} -c_x \\ c_y \end{Bmatrix}. \tag{3.19}$$

These limiting cases indicate that there is no 'predominantly torsional' long wave and there is no 'predominantly bending' short wave (the second eigenvector in equations (3.17) and (3.19). On the other hand, we do have a 'predominantly bending' long wave and a 'predominantly torsional' short wave (see the first eigenvector in equations (3.17) and (3.19)). The non-dispersive behaviour is usually attributed to torsional wave propagation. However, for the long wave under study, the non-dispersive propagation mode is truly mixed so long as c_y is finite. The case of $c_y \to 0$ is trivial, since it corresponds to the special situation of bending–torsion coupling being removed from the system, just as happens in rods with cross-sectional double symmetry. We observe from equations (3.16) and (3.18) that smaller the offset c_y, progressively greater is the 'pure' character of the propagating waves in these two extremes.

Interestingly the branch of dispersion curves that has purely bending character for long waves becomes the one with purely torsional character for short waves. The mid-wavenumber range sees the transition and it indeed has a mixed character.

Since the 'v equation' decouples from the 'w equation' and the 'ϕ equation' for double coupling, the bending–torsion coupled modes polarize along a principal direction of the cross-section. This means that (for example, the second mode in equations (3.16) and (3.18)) the cross-section rotates and moves up-down along the z-axis (which is a principal direction) *without* moving sideways along the y-axis. The pure bending mode (as in the first mode of (3.16)), of course, polarizes along this direction just as it does for classical bending waves.

The case of triple coupling is very similar, except that the planes of polarization can have a general inclination. The two mode shapes for long waves corresponding to the two branches described by equation (3.11) are purely bending waves in the limit $k \to 0$. The planes of polarization for these waves are the planes containing the principal axes. The mode shapes in the limit are obtained as

$$\lim_{k\to 0} \begin{Bmatrix} V \\ W \\ \Phi \end{Bmatrix}_{(1,2,3)} = \begin{Bmatrix} 0 \\ 1 \\ 0 \end{Bmatrix}, \begin{Bmatrix} 1 \\ 0 \\ 0 \end{Bmatrix}, \begin{Bmatrix} c_z \\ -c_y \\ 1 \end{Bmatrix}. \tag{3.20}$$

The third of these modes corresponds to the dispersion relation (3.12), which is non-dispersive in the limit of long waves. The propagation mode, however, is not the classical torsional dispersion, since it involves finite bending motions in both the y- and z-directions. The inclination of the plane of polarization of this coupled mode with respect to the y-axis is given by the arctangent of $-(c_y/c_z)$.

The propagation modes for short waves of a triply coupled rod can be found in a manner similar to that for the case of double coupling. Ignoring terms $O(1/k^2)$ and

smaller, in the limit of short waves we obtain

$$\lim_{k\to\infty}\left\{\begin{matrix}V\\W\\\Phi\end{matrix}\right\}_{(1,2,3)}=\left\{\begin{matrix}c_z r_{(1,2)}/(r_{(1,2)}-\lambda_\zeta)\\-c_y r_{(1,2)}/(r_{(1,2)}-\lambda_\eta)\\1\end{matrix}\right\},\left\{\begin{matrix}0\\0\\1\end{matrix}\right\}, \tag{3.21}$$

where r_1 and r_2 are the two coefficients of the leading term of the first equation in (3.13). Note that the planes of polarization are different from the principal planes, since both displacement components in the first two modes are non-zero.

4. Complex wavenumber and the λ-matrix problem

In the previous sections, real frequencies were determined for *real* wavenumber and *purely imaginary* wavenumber. The complete spectrum of the problem includes all wavenumbers—real, imaginary or complex—for specified real values of frequency. An exact solution is still possible, but a closed-form solution is not possible, for a general case. For a specified real value of frequency, the wavenumber can be calculated by reorganizing terms explicitly in terms of the unknown k:

$$[k^4\boldsymbol{A}_4+k^2\boldsymbol{A}_2+\boldsymbol{A}_0(\omega)]\boldsymbol{u}=\boldsymbol{0}. \tag{4.1}$$

Of the three coefficient matrices, $\boldsymbol{A}_4$ and $\boldsymbol{A}_2$ are constant matrices and depend on the cross-sectional geometry and material properties. The third matrix, $\boldsymbol{A}_0$, depends on the frequency, ω. Defining a new variable, $\sigma=k^2$, we have

$$[\sigma^2\boldsymbol{A}_4+\sigma\boldsymbol{A}_2+\boldsymbol{A}_0]\boldsymbol{u}=\boldsymbol{0}. \tag{4.2}$$

This is a λ-matrix problem (also known as the quadratic eigenproblem (see, for example, Lancaster 1966)) with σ as the parameter of the λ matrix. There are six possible non-trivial solutions for σ, but they cannot be obtained in closed form because an attempt to do so leads to a sixth-order algebraic equation. A more practical (and perhaps elegant) approach is to cast the λ-matrix problem (4.2) as a standard eigenproblem. The motivation for doing this stems from the fact that efficient eigensolvers are readily available on modern computing platforms.

Defining a 'state-vector' in a space spanned by the configurational variables vector $\boldsymbol{u}$ extended by $\sigma\boldsymbol{u}$, i.e.

$$\boldsymbol{w}=[\boldsymbol{u}^{\mathrm{T}}|\sigma\boldsymbol{u}^{\mathrm{T}}]^{\mathrm{T}}, \tag{4.3}$$

we can express the λ-matrix problem as the following standard eigenvalue problem

$$\mathcal{D}\boldsymbol{w}=\sigma\boldsymbol{w}. \tag{4.4}$$

Note that the eigenvalues σ of (4.4) are the same as the latent roots of the λ matrix in (4.2). The 6×6 matrix $\mathcal{D}$ is given by

$$\mathcal{D}=\begin{bmatrix}\boldsymbol{0} & \boldsymbol{I}\\ -(\boldsymbol{A}_4^{-1}\boldsymbol{A}_0) & (\boldsymbol{A}_4^{-1}\boldsymbol{A}_2)\end{bmatrix}. \tag{4.5}$$

The eigenvalues σ can be real or complex. The value of the wavenumber is calculated by taking the square root of σ when it is real. When $\sigma=r\exp(\pm\mathrm{i}\theta)$ is complex, the wavenumber is given by $k=\pm\sqrt{r}\exp(\pm\mathrm{i}\theta/2)$.

For the case of double coupling, a closed-form solution is still possible for the complete spectrum. One equation of (4.2) now decouples from the remaining two; the resulting λ-matrix problem has as its determinant a *quartic* in σ, and hence has a closed-form solution.

If material damping is to be included in the model, the equations of motion (2.3) are modified. The dispersion relation (4.1) is modified accordingly. For example, if viscous damping is used in the model, $\boldsymbol{A}_0(\omega)$ becomes complex and is replaced by, say, $\boldsymbol{A}_0(\omega) + \mathrm{i}\omega\boldsymbol{C}$, where $\boldsymbol{C}$ is the damping matrix. Alternatively, if a 'complex elastic modulus' model is used (in the frequency domain), then $\boldsymbol{A}_2$ and $\boldsymbol{A}_4$ need to be replaced by complex matrices. The eigenproblem (4.4) still provides the complete dispersion spectrum.

5. Numerical examples and discussions

As an illustrative example, we take the data from Yaman (1997) for a cross-section that exhibits triple-coupling. The cross-sectional and material properties are given as

$$\begin{aligned}
h &= 38.1 \times 10^{-3}\ \mathrm{m}, & A &= 9.68 \times 10^{-5}\ \mathrm{m}^2, & I_{z'} &= 5.08 \times 10^{-9}\ \mathrm{m}^4,\\
I_{y'} &= 2.24 \times 10^{-8}\ \mathrm{m}^4, & I_{y'z'} &= 4.25 \times 10^{-9}\ \mathrm{m}^4, & c_{y'} &= 10.43 \times 10^{-3}\ \mathrm{m},\\
c_{z'} &= 9.09 \times 10^{-3}\ \mathrm{m}, & C &= 5.2 \times 10^{-11}\ \mathrm{m}^4, & I_0 &= 4.6 \times 10^{-8}\ \mathrm{m}^4,\\
\rho &= 2700\ \mathrm{kg\,m}^{-3}, & E &= 7 \times 10^{10}\ \mathrm{N\,m}^{-2}, & G &= 2.6 \times 10^{10}\ \mathrm{N\,m}^{-2},\\
& & C_w &= 7.11 \times 10^{-12}\ \mathrm{m}^6, & &
\end{aligned}$$

and h is used as a characteristic length for the cross-section. Results will be presented for the non-dimensional wavenumber and the non-dimensional frequency, defined as

$$k^* = hk \quad \text{and} \quad \omega^* = h^2\left(\frac{\rho A}{EI_M}\right)^{1/2}\omega, \tag{5.1}$$

where I_M is a characteristic second moment of area given by $I_M = \max(I_\zeta, I_\eta)$ and (ζ, η) are the principal directions. The coordinates of the centroid of the cross-section (c_y, c_z) are obtained by rotating the vector $(c_{y'}, c_{z'})$ using the transformation that diagonalizes the second moment of the area tensor.

The example of double coupling is contrived by setting $c_{y'} = 0$ and $I_{y'z'} = 0$ in the data given above. When warping is ignored, the closed-form analytical solutions are presented using the dots in figure 1. Of the three branches, the one that exactly matches the solid line connecting circles is decoupled from torsion and bending about the y'-axis and corresponds to classical bending about z'-axis which is parabolic for all wavenumbers (branch labelled 'classical bending (decoupled)'). The other two propagating waves have, in general, a mixed bending–torsion character. The lower branch (parabolic for long waves and linear for short waves) has the two classical waves as the asymptotes (solid lines and circles): long waves for this branch are dispersive and have a dominant bending nature, whereas short waves are non-dispersive and have a dominant torsional character. The third branch (the set of little dots above all other curves in the figure) represents *non-dispersive* propagation for long waves and dispersive propagation for short waves, the two lines connecting diamonds being the respective asymptotes (the straight line for long waves and the

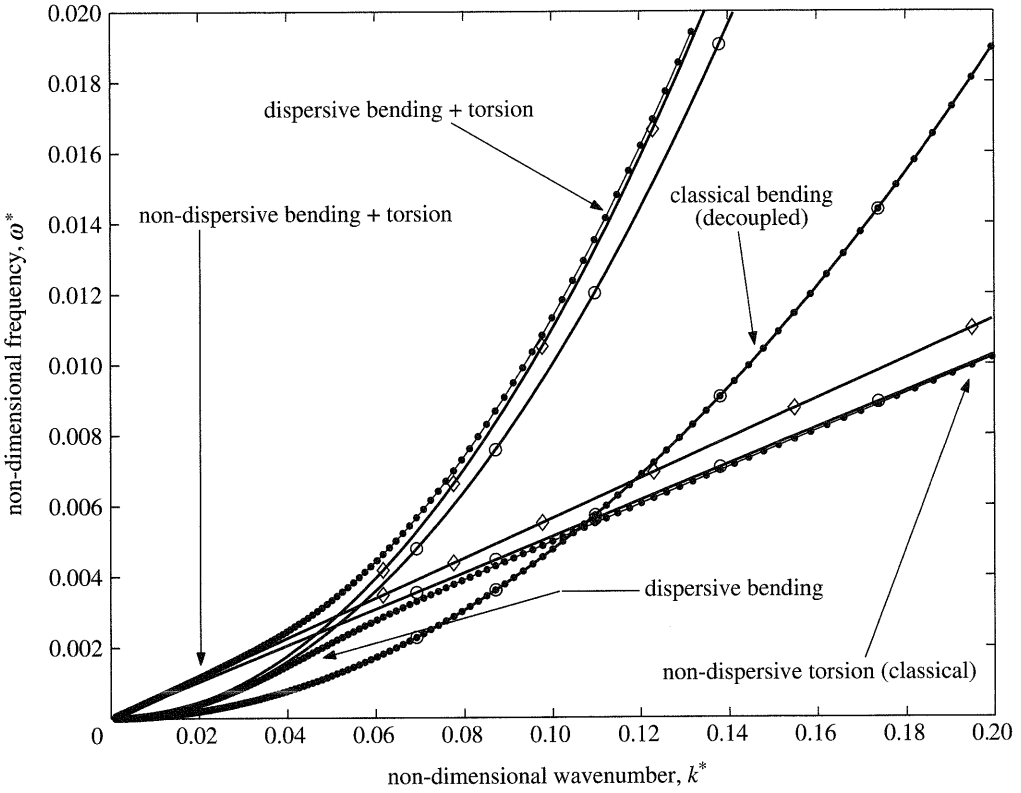

Figure 1. Dispersion curves for the case of double coupling when $c_y = 0$. The solid lines with circles in each case correspond to the three classical waves: two bending and one torsion. The solid lines with diamond markers are asymptotes with mixed bending–torsion character. The dots joined by solid lines represent the three branches of the closed-form analytical solution.

parabola for short waves). In spite of the non-dispersive nature of propagation for long waves associated with this branch, the waveguide mode is not torsional in the long-wavelength limit: this branch is truly of a mixed bending–torsion character for all regimes of wavelengths. Note that the three solid lines connecting circles have been obtained by ignoring the coupling terms in the bending–torsion equations.

When $c_{z'} = I_{y'z'} = 0$, the bending wave corresponding to bending about the y'-axis is decoupled to the remaining two motions of the cross-section (bending about the z'-axis and torsion). One obtains a similar set of curves to those in figure 1; these curves are not reported here.

The two solid lines connecting circles in figure 1 (the straight line for torsion and the parabola for bending) intersect each other and they correspond to decoupled bending and torsional motion. The dots, on the other hand, do not cross each other. The dotted curve corresponding to the classical bending that is decoupled from other cross-sectional motions does not veer against any of this pair of mutually veering lines. The phenomenon of 'curve veering' or 'eigenvalue loci veering' has been reported in the context of curves that represent the values of frequency as a function of structural parameter (e.g. a length, mass, thickness, etc.) by many authors (see, for example, Perkins & Mote 1986; Pierre 1988). Eigenvalue loci veering in case of

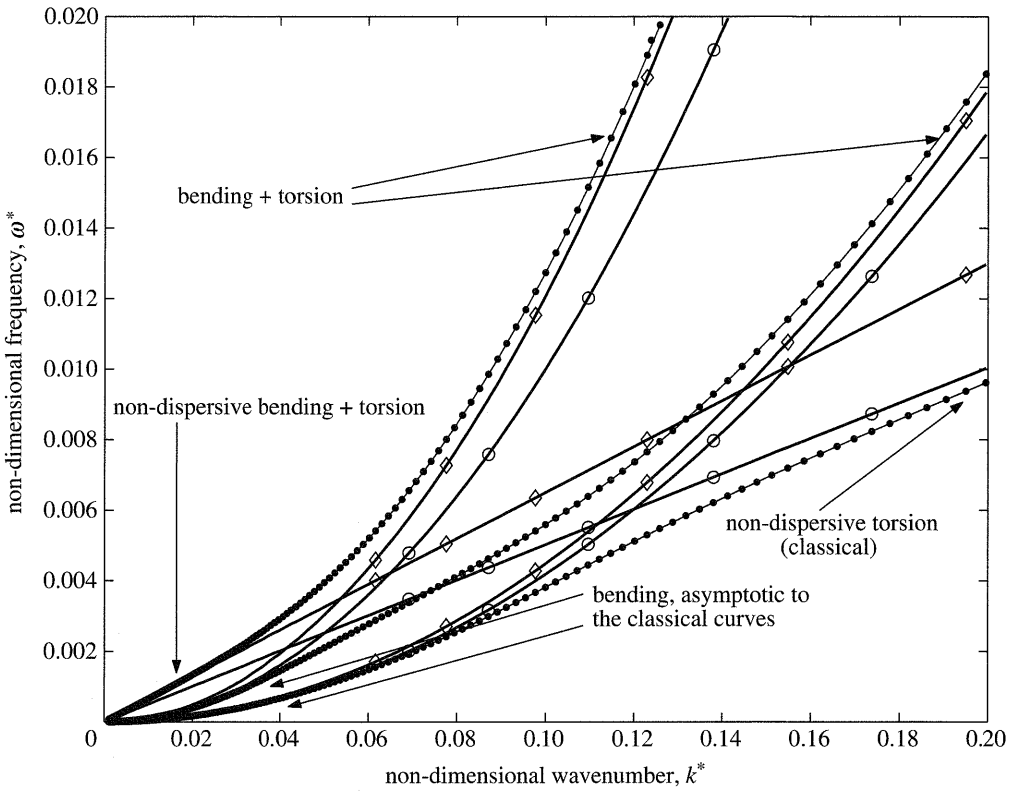

Figure 2. Dispersion curves for the case of triple coupling. The solid lines with circles in each case correspond to the three classical waves: two bending and one torsion. The solid lines with diamond markers are asymptotes with mixed bending–torsion character. The dots joined by solid lines represent the three branches of the closed-form analytical solution.

free vibration is observed when two frequencies come close to each other (but never become degenerate) when a system parameter is varied. In the present case of the veering of the dispersion curves, the wavenumber has the same mathematical role as a system parameter has in the case of discrete vibratory systems.

When both c_y and c_z are non-zero, the two bending waves and the torsional wave are triply coupled. The dispersion curves are shown in figure 2 for the numerical data given above. The lowest curve connecting dots shows dispersive bending behaviour for long waves and non-dispersive torsional behaviour for short waves; the character is mixed for intermediate wavelengths. The two solid lines connecting circles corresponding to the classical decoupled waves for bending about the z-axis and torsion are the asymptotes for long and short waves, respectively. The upper curve shows a *non-dispersive* mixed bending–torsion behaviour for long waves and dispersive mixed behaviour for short waves. The middle line connecting dots shows pure bending behaviour for long waves but has a mixed character for short waves.

When warping is included in the model, we do not expect any change in the asymptotic behaviour for long waves. Hence, for the case of double coupling (see figure 3), the bottom left-hand corner resembles that of figure 1. For short waves, pure torsion is dispersive when warping is included—this is seen at the right-hand

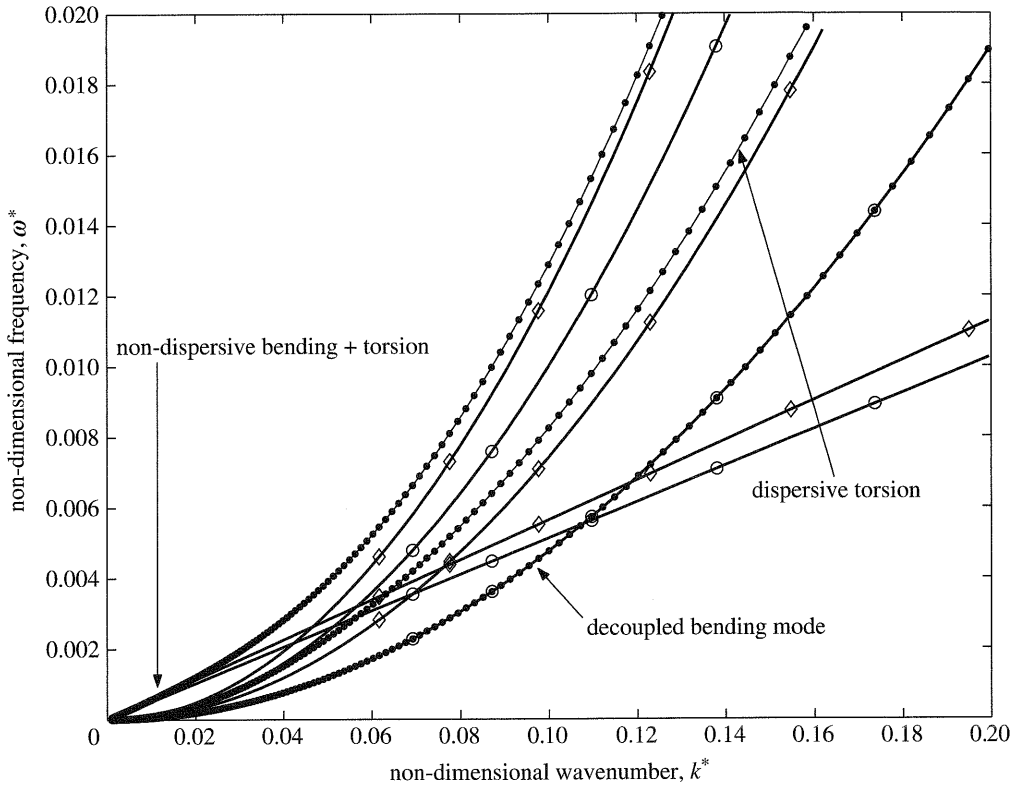

Figure 3. Dispersion curves for the case of double coupling when $c_y = 0$ and warping deformations are included in the model. The solid lines with circles in each case correspond to the three classical waves: two bending and one torsion. The solid lines with diamond markers are asymptotes with mixed bending–torsion character. The dots joined by solid lines represent the three branches of the closed-form analytical solution.

end of the line connecting dots that is asymptotic to the parabola corresponding to torsion. It includes warping as the dominant stiffness effect. Bending about the z-axis is decoupled as before.

As a last example, consider the case of triple coupling for the same data as before (i.e. the one that produced figure 2) *plus* warping. The objective now is to calculate all the admissible values of wavenumber for given real values of frequency. The 12 values of wavenumber for each frequency are presented in figure 4. There are six lines: the three lines labelled 'propagating waves' correspond to progressive waves. The remaining three lines correspond to evanescent waves. The curves are not joined because the order in which the eigenvalues are calculated numerically do not stay unchanged; an attempt to join them in an automated way proves to be unnecessarily complicated. The three propagating waves correspond to the three pairs of real values of the wavenumber (they come in pairs of opposite sign). The three evanescent waves correspond to the three imaginary values of the wavenumber for each real frequency, again in pairs of opposite sign (the three branches that are not labelled 'propagating waves'). The upper line for propagating waves has a bending character for low frequencies and a dispersive torsional character for high frequencies (due

to the dominant warping effect for short waves). The portion of the curve in the mid-frequency regime represents a mixed bending–torsional character.

The lower curve has a *non-dispersive* mixed character for low frequencies and this gradually becomes more and more dispersive; the motion is truly mixed for all regimes of frequencies. The fact that the waveguide mode is not purely torsional (despite the $\omega(k)$ relation being linear) can be checked from the corresponding eigenvector close to the origin on this branch of the dispersion curve. The numerically calculated eigenvector is obtained as $(-0.8105, 0.5858, 1)$ after the displacement coordinates have been non-dimensionalized by a factor $1/(c_y^2 + c_z^2)^{1/2}$. This compares well with the analytical result of the third eigenvector in equation (3.20), similarly non-dimensionalized,

$$\left(\frac{c_z}{\sqrt{c_y^2 + c_z^2}}, \frac{-c_y}{\sqrt{c_y^2 + c_z^2}}, 1\right) = (-0.8105, 0.5858, 1).$$

Therefore, the mode has comparable magnitude of bending and torsional components; when the quantities of actual physical dimensions (two displacements and an angle) are used, it becomes difficult to make such a comparison.

In the limit of long waves, the plane of polarization is inclined at an angle

$$\tan^{-1}\frac{W}{V} = \tan^{-1}\frac{0.5858}{-0.8105} \approx -36^\circ$$

to the y-axis. For other wavenumber values, the inclination of the polarization plane can be calculated by the use of equation (3.15).

The third dispersion curve for propagating waves stays in the middle and has a purely bending character for low frequencies (and long waves); this motion progressively becomes mixed bending–torsional motion as the frequency increases.

The two evanescent waves have bending behaviour at low frequencies; this becomes mixed motion as the frequency increases. The upper curve has a curious behaviour: it has a cut-on on the k-axis indicating that this evanescent wave exists only for waves shorter than a certain length. For the numerical data considered here, the value of cut-on is 0.0628. This could be explained by a simple analysis; consider equation (2.5) in the limit $\omega \to 0$. The three equations are decoupled in this limit and the limiting wavenumber values are given by $k^4\lambda_\zeta = 0$, $k^4\lambda_\eta = 0$ and $k^4\lambda_w + k^2\lambda_\mathrm{p} = 0$. The first two of these equations correspond to the dispersive bending branches of the propagating and the evanescent waves. The third equation has a root $k = 0$, which corresponds to the non-dispersive bending–torsion wave in the limit of long waves. The second set of roots of the third equation is $k^* = kh = \pm ih\sqrt{\lambda_\mathrm{p}/\lambda_w} = 0.0628$; these values correspond to the cut-on point on the wavenumber axis.

While figure 4 brings out features of the dispersion relation for long waves at low frequency well, the picture for a wider range of wavenumber is given better when logarithmic axes (both for frequency and wavenumber) are used (see figure 5). For non-dispersive propagation, the slope on a log-log scale is unity (one decade on the ordinate corresponds to one decade on the abscissa). This is exhibited by the lowest of the six curves. For propagation of the type $\omega \sim k^2$ (classical bending, warping-dominated torsion and short-wave mixed-mode propagation), the slope is seen to be 0.5 (one decade on the ordinate corresponds to two decades on the abscissa). This is correctly illustrated by the curves at the right-hand end of the figure. Again the cut-on on the y-axis occurs at $k^* = 0.0628$.

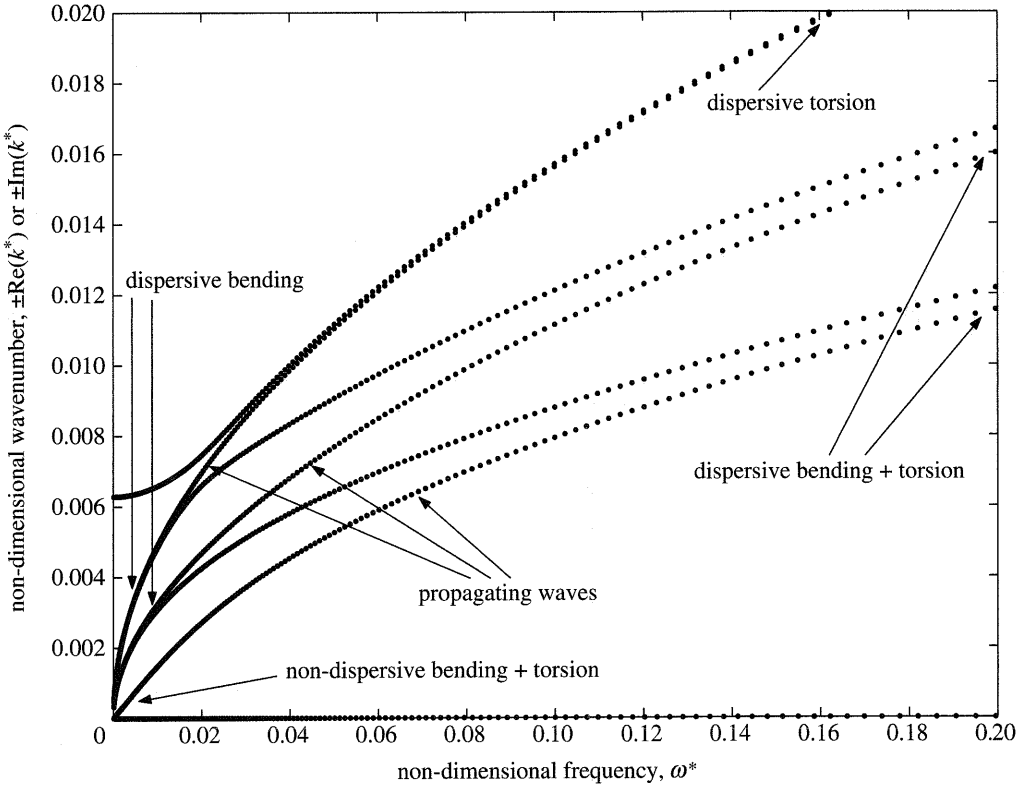

Figure 4. Complete spectrum for the case of triple coupling. Warping deformations are included in the model. Note the linear region in the lowest curve near the origin indicating a non-dispersive behaviour.

Figure 5 may be compared with fig. 10 of Yaman (1997). There is a general agreement between the two, except that the cut-on frequency in case of Yaman's paper is 0.0346, since the warping constant used by him was 2.334×10^{-11} and not 7.11×10^{-12} as misquoted there (this was clarified by Yaman through the editor of *Proceedings of the Royal Society of London* Series A in a personal communication.).

6. Conclusions

Wave propagation in elastic rods with bending–torsion coupling was studied analytically. For the general case of triple coupling, the propagating and the evanescent waves were obtained as a solution to a cubic equation. For cross-sections with one axis of symmetry (i.e. for the case of double coupling), this results in a quadratic equation.

In the limits of short and long waves, the frequency–wavenumber relationship and the waveguide propagation modes were obtained as asymptotic expansions. The case of long waves results in a problem of regular perturbation, whereas the case of short waves results in a problem of singular perturbation with the reciprocal of the wavenumber as a suitable 'small' parameter. The cases of double and triple coupling were considered with and without warping being included in the model.

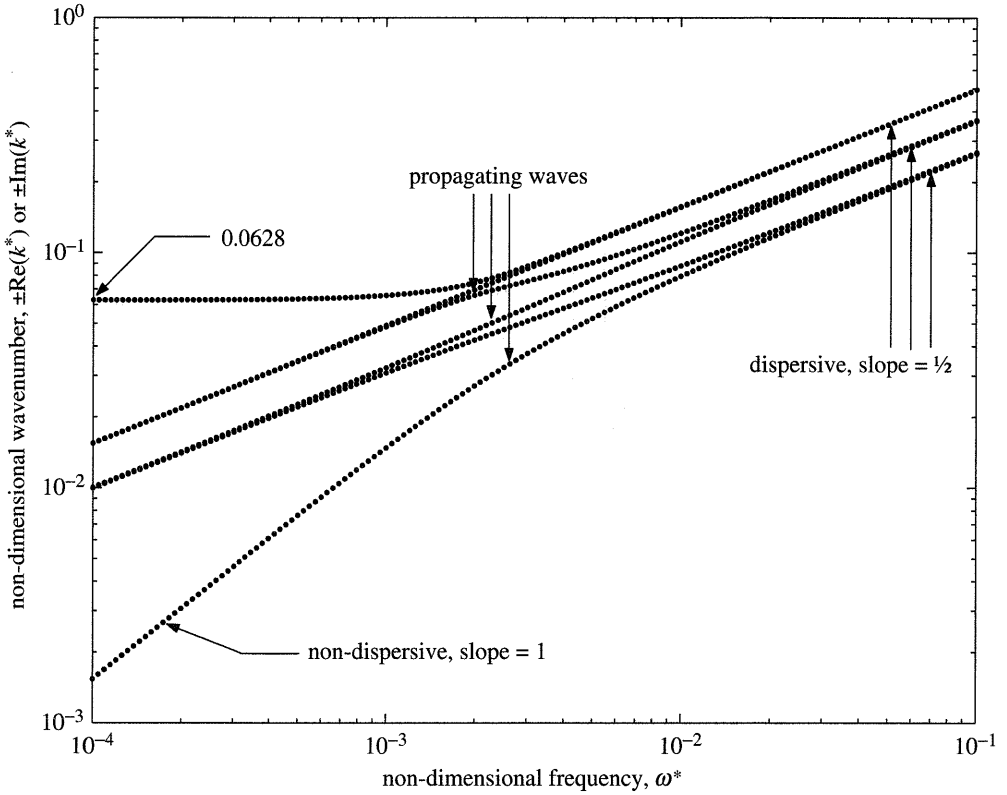

Figure 5. Complete spectrum for the same case as in figure 4. All the lines become asymptotically dispersive with wavenumber being proportional to the square of frequency: on a log–log plot they are straight lines with one decade on the ordinate corresponding to two decades on the abscissa. At low frequencies, the lowest curve shows non-dispersive behaviour: one decade on the ordinate corresponds to one decade on the abscissa.

For double coupling without warping, one branch of the dispersion curve has classical bending behaviour for long waves and classical torsional behaviour for short waves. The intermediate values of the wavenumber have a mixed bending–torsion character. The second branch has a mixed bending–torsion character for all regimes of the wavenumber—this is despite an asymptotically non-dispersive frequency–wavenumber relationship for long waves. The third branch is decoupled and represents classical bending in the plane spanned by the propagation direction and the axis of symmetry. For the case of triple coupling, the third branch of the dispersion curve has an asymptotically bending character for long waves but it represents mixed bending–torsion motion for short waves. When warping is included in the model, short waves become dispersive for purely torsional motion (as in the first branch); the long-wave asymptotes are unaffected, as expected.

It was observed that coupled bending–torsion motion is associated with two well-known phenomena: polarization and eigenvalue loci veering. Perhaps this problem affords the simplest example that illustrates these phenomena in the context of elastic wave propagation.

Numerical results are in agreement with the asymptotic analyses presented in this paper for various cases of coupling in various propagation regimes.

Thanks are due to my colleagues Dr Chris Howls, Dr Neil Stephen and Mr David Stinchcombe for useful discussions; to Y. Yaman for communicating to me through the editor of this journal that the value of the warping constant was misquoted in his paper and for kindly supplying figures with greater resolution; and finally, to the referees for their comments.

References

Bishop, R. E. D. & Price, W. G. 1977 Coupled bending and twisting of a Timoshenko beam. *J. Sound Vib.* **50**, 469–477.

Bishop, R. E. D., Price, W. G. & Xi-Cheng, Z. 1985 A note on the dynamical behaviour of uniform beams having open channel section. *J. Sound Vib.* **99**, 155–167.

Bishop, R. E. D., Cannon, S. M. & Miao, S. 1989 On coupled bending and torsional vibration of uniform beams. *J. Sound Vib.* **131**, 457–464.

Dokumaci, E. 1987 An exact solution for coupled bending and torsion vibrations of uniform beams having single cross-sectional symmetry. *J. Sound Vib.* **119**, 443–449.

Gere, J. M. & Lin, Y. K. 1958 Coupled vibrations of thin-walled beams of open cross-section. *ASME J. Appl. Mech.* **80**, 373–378.

Graff, K. F. 1975 *Wave motion in elastic solids.* New York: Dover.

Lancaster, P. 1966 *Lambda-matrices and vibrating systems.* New York: Pergamon.

Lin, Y. K. 1960 Coupled vibrations of restrained thin-walled beams. *ASME J. Appl. Mech.* **82**, 739–740.

Nayfeh, A. H. 1973 *Perturbation methods.* Wiley.

Nickalls, R. W. D. 1993 A new approach to solving the cubic: Cardan's solution revealed. *Math. Gazette* **77**, 354–359.

Perkins, N. C. & Mote, C. D. 1986 Comments on curve veering in eigenvalue problems. *J. Sound Vib.* **106**, 451–463.

Pierre, C. 1988 Mode localization and eigenvalue veering phenomena in disordered periodic structures. *J. Sound Vib.* **126**, 485–502.

Timoshenko, S. 1955 *Vibration problems in engineering.* New York: Van Nostrand.

Yaman, Y. 1997 Vibrations of open-section channels: a coupled flexural and torsional wave analysis. *J. Sound Vib.* **204**, 131–158.